

2f

PNL-4490
UC-70

Recycle of Iodine-Loaded Silver Mordenite by Hydrogen Reduction

L. L. Burger
R. D. Scheele

November 1982

Prepared for the U.S. Department of Energy
under Contract DE-AC06-76RLO 1830

Pacific Northwest Laboratory
Operated for the U.S. Department of Energy
by Battelle Memorial Institute



PNL-4490

DISCLAIMER

This report was prepared as an account of work sponsored by an agency of the United States Government. Neither the United States Government nor any agency thereof, nor any of their employees, makes any warranty, express or implied, or assumes any legal liability or responsibility for the accuracy, completeness, or usefulness of any information, apparatus, product, or process disclosed, or represents that its use would not infringe privately owned rights. Reference herein to any specific commercial product, process, or service by trade name, trademark, manufacturer, or otherwise, does not necessarily constitute or imply its endorsement, recommendation, or favoring by the United States Government or any agency thereof. The views and opinions of authors expressed herein do not necessarily state or reflect those of the United States Government or any agency thereof.

PACIFIC NORTHWEST LABORATORY
operated by
BATTELLE
for the
UNITED STATES DEPARTMENT OF ENERGY
under Contract DE-AC06-76RLO 1830

Printed in the United States of America
Available from
National Technical Information Service
United States Department of Commerce
5285 Port Royal Road
Springfield, Virginia 22151

NTIS Price Codes
Microfiche A01

Printed Copy

Pages	Price Codes
001-025	A02
026-050	A03
051-075	A04
076-100	A05
101-125	A06
126-150	A07
151-175	A08
176-200	A09
201-225	A010
226-250	A011
251-275	A012
276-300	A013

PNL-4490
UC-70

RECYCLE OF IODINE-LOADED SILVER
MORDENITE BY HYDROGEN REDUCTION

L. L. Burger
R. D. Scheele

November 1982

Prepared for
the U.S. Department of Energy
under Contract DE-AC06-76RL0-1830

Pacific Northwest Laboratory
Richland, Washington 99352

.

'

'

'

'

'

'

'

SUMMARY

In 1977 and 1978, workers at Idaho National Engineering Laboratory (INEL) developed and tested a process for the regeneration and reuse of silver mordenite, AgZ, used to trap iodine from the dissolver off-gas stream of a nuclear fuel reprocessing plant. We were requested by the Airborne Waste Management Program Office of the Department of Energy to perform a confirmatory recycle study using repeated loadings at about 150°C with elemental iodine, each followed by a drying step at 300°C, then by iodine removal using elemental hydrogen at 500°C.

The results of our study show that AgZ can be recycled. There was considerable difficulty in stripping the iodine at 500°C; however, this step went reasonably well at 550°C or slightly higher, with no apparent loss in the iodine-loading capacity of the AgZ.

Large releases of elemental iodine occurred during the drying stage and the early part of the stripping stage. Lead zeolite, which was employed in the original design to trap the HI produced, is ineffective in removal of I₂. The process needs modification to handle the iodine.

Severe corrosion of the stainless steel components of the system resulted from the HI-I₂-H₂O mixture. Monel® or other halogen-resistant materials need to be examined for this application.

Because of difficulty with the stripping stage and with corrosion, the experiments were terminated after 12 cycles. Thus, the maximum lifetime (cycles) of recycled AgZ has not been determined.

Mechanistic studies of iodine retention by silver zeolites and of the behavior of silver atoms on the reduction stage would be of assistance in optimizing silver mordenite recycle.

®Trademark of Huntington Alloys, Inc., Huntington, West Virginia.

•
•
•
•

•
•
•
•

CONTENTS

SUMMARY	iii
INTRODUCTION	1
CONCLUSIONS AND RECOMMENDATIONS	3
EXPERIMENTAL ELEMENTS	5
RESULTS	9
DISCUSSION	15
ACKNOWLEDGMENTS	21
REFERENCES	23
APPENDIX	A.1

•
•
•
•

•
•
•
•

FIGURES

1	Iodine Loading and Stripping Experimental Apparatus	6
2	Stereo View of Sodium Mordenite	15
3	Scanning Electron Micrograph of 100 mg I/g Ag ^o Z	17

TABLES

1	Zeolite Bed Descriptions	8
2	Experimental Operating Conditions for AgZ and PbX Beds During Iodine Loading and AgZ Recycle	8
3	Summary of Iodine Loading and Stripping	10
A.1	Iodine-Loading Characteristics for AgZ Bed 1, Cycle 1, Loading Stage	A.1
A.2	Iodine-Loading Characteristics for AgZ Bed 1, Cycle 1, Drying Stage	A.1
A.3	Iodine-Loading Characteristics for AgZ Bed 1, Cycle 2, Loading Stage	A.2
A.4	Iodine-Loading Characteristics for AgZ Bed 2, Cycle 1, Loading Stage	A.3
A.5	Iodine-Loading Characteristics for AgZ Bed 2, Cycle 1, Drying Stage	A.3
A.6	Iodine-Loading Characteristics for AgZ Bed 2, Cycle 2, Loading Stage	A.4
A.7	Iodine-Loading Characteristics for AgZ Bed 2, Cycle 2, Drying Stage	A.4
A.8	Iodine-Loading Characteristics for AgZ Bed 2, Cycle 2, Stripping Stage	A.5
A.9	Iodine-Loading Characteristics for AgZ Bed 2, Cycle 3, Loading Stage	A.6
A.10	Iodine-Loading Characteristics for AgZ Bed 2, Cycle 3, Drying Stage	A.6
A.11	Iodine-Loading Characteristics for AgZ Bed 2, Cycle 3, Stripping Stage	A.7
A.12	Iodine-Loading Characteristics for AgZ Bed 2, Cycle 4, Loading Stage	A.8

TABLES (Continued)

A.13	Iodine-Loading Characteristics for AgZ Bed 2, Cycle 4, Drying Stage	A.8
A.14	Iodine-Loading Characteristics for AgZ Bed 2, Cycle 4, Stripping Stage	A.9
A.15	Iodine-Loading Characteristics for AgZ Bed 2, Cycle 5, Loading Stage	A.10
A.16	Iodine-Loading Characteristics for AgZ Bed 2, Cycle 5, Drying Stage	A.10
A.17	Iodine-Loading Characteristics for AgZ Bed 2, Cycle 5, Stripping Stage	A.11
A.18	Iodine-Loading Characteristics for AgZ Bed 2, Cycle 6, Loading Stage	A.12
A.19	Iodine-Loading Characteristics for AgZ Bed 2, Cycle 6, Drying Stage	A.12
A.20	Iodine-Loading Characteristics for AgZ Bed 2, Cycle 6, Stripping Stage	A.13
A.21	Iodine-Loading Characteristics for AgZ Bed 2, Cycle 7, Loading Stage	A.14
A.22	Iodine-Loading Characteristics for AgZ Bed 2, Cycle 7, Drying Stage	A.14
A.23	Iodine-Loading Characteristics for AgZ Bed 2, Cycle 7, Stripping Stage #1	A.15
A.24	Iodine-Loading Characteristics for AgZ Bed 2, Cycle 7, Stripping Stage #2	A.15
A.25	Iodine-Loading Characteristics for AgZ Bed 2, Cycle 8, Loading Stage	A.16
A.26	Iodine-Loading Characteristics for AgZ Bed 2, Cycle 8, Drying Stage	A.16
A.27	Iodine-Loading Characteristics for AgZ Bed 2, Cycle 8, Stripping Stage	A.17
A.28	Iodine-Loading Characteristics for AgZ Bed 2, Cycle 9, Loading Stage	A.18
A.29	Iodine-Loading Characteristics for AgZ Bed 2, Cycle 9, Drying Stage	A.18

TABLES (Continued)

A.30	Iodine-Loading Characteristics for AgZ Bed 2, Cycle 9, Stripping Stage	A.19
A.31	Iodine-Loading Characteristics for AgZ Bed 2, Cycle 10, Loading Stage	A.20
A.32	Iodine-Loading Characteristics for AgZ Bed 2, Cycle 10, Drying Stage	A.20
A.33	Iodine-Loading Characteristics for AgZ Bed 2, Cycle 10, Stripping Stage	A.21
A.34	Iodine-Loading Characteristics for AgZ Bed 2, Cycle 11, Loading Stage	A.22
A.35	Iodine-Loading Characteristics for AgZ Bed 2, Cycle 11, Drying Stage #1	A.22
A.36	Iodine-Loading Characteristics for AgZ Bed 2, Cycle 11, Stripping Stage #1	A.23
A.37	Iodine-Loading Characteristics for AgZ Bed 2, Cycle 11, Drying Stage #2	A.23
A.38	Iodine-Loading Characteristics for AgZ Bed 2, Cycle 11, Stripping Stage #2	A.24
A.39	Iodine-Loading Characteristics for AgZ Bed 2, Cycle 11, Stripping Stage #3	A.24
A.40	Iodine-Loading Characteristics for AgZ Bed 2, Cycle 12, Loading Stage	A.25
A.41	Iodine-Loading Characteristics for AgZ Bed 2, Cycle 12, Drying Stage	A.25
A.42	Iodine-Loading Characteristics for AgZ Bed 2, Cycle 12, Stripping Stage #1	A.26
A.43	Iodine-Loading Characteristics for AgZ Bed 2, Cycle 12, Stripping Stage #2	A.26
A.44	Iodine-Loading Characteristics for AgZ Bed 2, Cycle 12, Stripping Stage #3	A.27
A.45	Iodine-Loading Characteristics for AgZ, Bed 2, Cycle 12, Stripping Stage #4	A.27

.

.

.

.

.

.

.

.

INTRODUCTION

Silver-exchanged zeolites, especially silver mordenite, AgZ, have received considerable attention as agents for removal of radioactive iodine species from gas streams. Although it is marginally suitable as a final disposal form (Burger, Scheele and Wiemers 1981), the value of silver has prompted some effort in recycling the silver mordenite by removal of the iodine. Workers at Idaho National Engineering Laboratory (INEL) (Thomas et al. 1977; Murphy, Staples and Thomas 1977) carried out a series of iodine loadings followed by removal by hydrogen. This work was summarized by Thomas and a conceptual process described (Thomas, Staples and Murphy 1978). With an iodine loading corresponding to about 34% silver utilization, no decrease in capacity was observed over 5 cycles, a 20% decrease after 13 cycles. By contrast, silver faujasite, AgX, was noticeably degraded after 5 cycles.

As part of our iodine fixation program, we were asked to carry out a confirmatory recycle test using repeated loadings with elemental iodine, each followed first by a drying step, then by iodine removal using elemental hydrogen. This study is presented here.



CONCLUSIONS AND RECOMMENDATIONS

Based on our studies of hydrogen regeneration of iodine-loaded silver mordenite (AgZI), we conclude that silver mordenite (AgZ) can be reused for iodine capture from a nuclear fuels reprocessing plant's dissolver off-gas stream. For employment of this process, provision must be made for control of elemental iodine released during the drying and stripping stages; also, materials of construction resistant to the I_2 -HI- H_2O triad must be determined. We believe that mechanistic studies of the iodine capture and stripping processes are very desirable.

In this study, a 320 g AgZ bed (5 cm dia. x 20 cm) was loaded and stripped a total of 12 times. The loading levels and bed behavior on drying and stripping varied with each cycle. The iodine loaded per cycle ranged from 60 to 125 mg I/g AgZ, with an average of 86 mg I/g AgZ; the total iodine loadings ranged from 96 to 200, with an average of 144 mg I/g AgZ. The maximum theoretical loading (based on the silver content of the zeolite) is 225 mg I/g AgZ.

During drying and the early stages of hydrogen treatment, considerable elemental iodine was released from the bed. This I_2 was not captured by the lead zeolite X (PbX) bed; it either circulated throughout the recycle system or was deposited onto the AgZ bed or various components of the system. Iodine in the system loop caused occasional plugging of valves and enhanced the corrosion of the stainless steel components of the system.

Success in removing the iodine from the AgZ varied from cycle to cycle. Beginning with the 5th cycle, we were unable to remove all the loaded iodine, which subsequently accumulated with each successive cycle until run 11. After a multiple stripping of loading 11, we had reduced the iodine content from 140 mg I/g AgZ (after cycle 10) to 21 mg I/g AgZ. Upon closer analysis of the different cycles, it appears that a temperature of 550°C or greater is required to effectively strip the iodine.

Corrosion of the stainless steel components in our system was a major problem. In particular, the stainless steel bellows of the recirculating pump

failed frequently from corrosion. If recycling is considered further, then other materials of construction, such as Monel®, need to be considered.

The release of I₂ upon heating suggests an alternative process using air or N₂ and heating at 400-600°C to remove the 60-80% of the iodine which is not strongly bound. The released iodine could then be captured in an aqueous hydroxide trap.

Our brief examination of the chemistry of iodine on silver zeolites shows gaps in the basic information. Of importance to the present study are such things as the bonding of molecular iodine in the zeolite and the location of silver atoms and their migration during reduction.

®Trademark of Huntington Alloys, Inc., Huntington, West Virginia.

EXPERIMENTAL ELEMENTS

The loading and stripping apparatus used is diagrammed in Figure 1. The containers for the AgZ (silver mordenite) and PbX (lead zeolite X) were constructed of 50 mm I.D. quartz and borosilicate glass, respectively. Each was heated with a large tube furnace. Three thermocouple wells were evenly spaced over the 20 cm, packed, AgZ bed length. The iodine generator and associated ports, as well as the condensers for water removal, were borosilicate glass. All other components, including the 13 mm connecting lines, were stainless steel, predominately type 316. A Datatest Corporation^(a) Model 301 oxygen detector was employed during the drying and hydrogenation stages. It registered 0-25% with a logarithmic response curve giving high accuracy at low concentrations.

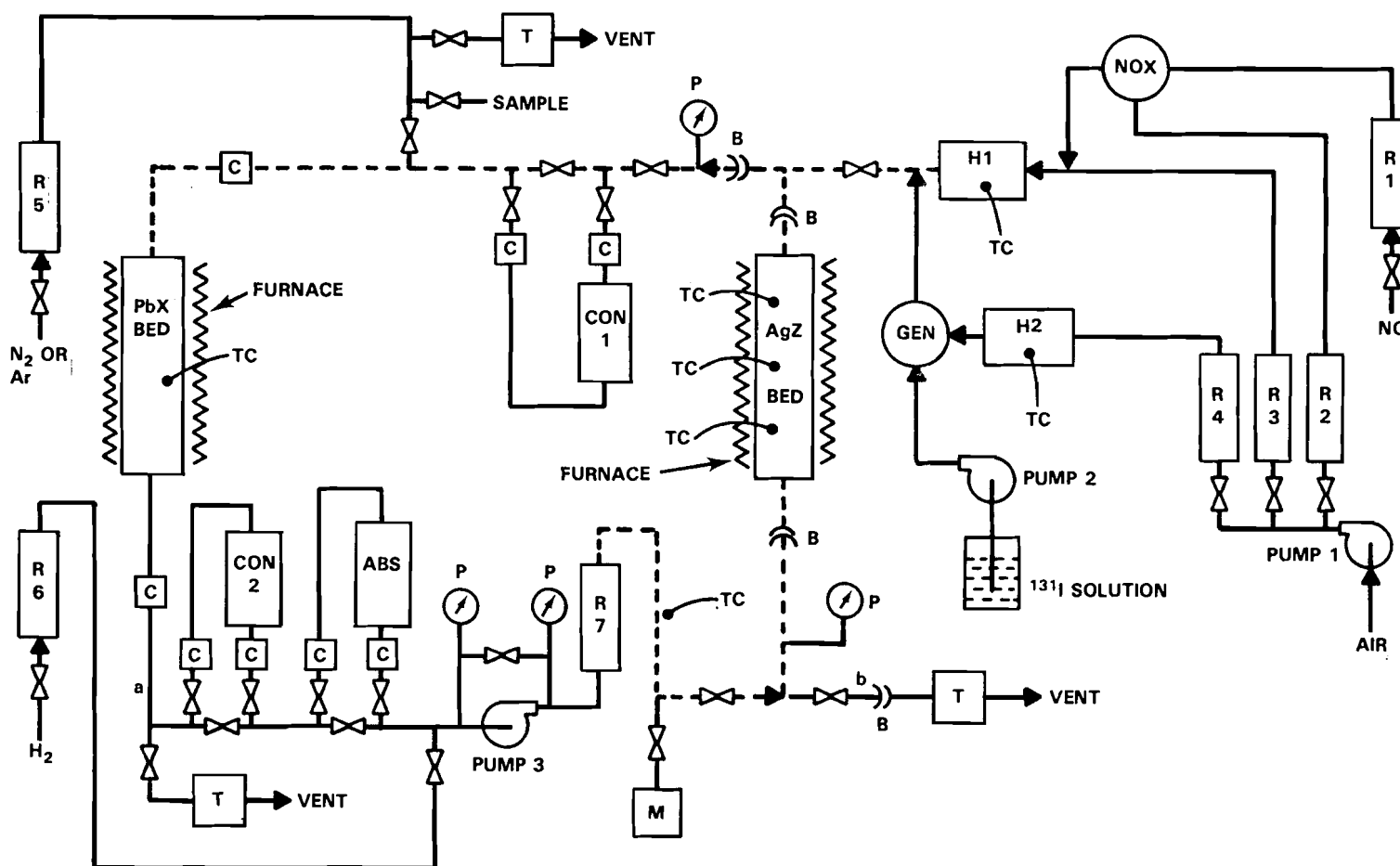
The iodine generator used the $I^- + IO_3^-$ reaction in the presence of 4 M H_2SO_4 . Potassium iodide traced with ^{131}I was pumped into the $IO_3^- - H_2SO_4$ solution with the metering pump, Pump No. 1, and the resulting I_2 was swept into the AgZ bed with warmed air. The 1 liter hold-up bulb was operated with a residence time calculated to convert approximately 50% of the NO to NO_2 .

A cycle consisted of 4 stages: pretreatment, iodine loading, drying, and hydrogen reduction or stripping. Pretreatment consisted of a short treatment with room air at 150°C to re-equilibrate the AgZ with respect to moisture.

For the loading stage, breakthrough was best determined by using a layer of AgX in a tube at the outlet, point a. Experience showed that the AgX turned yellow when the decontamination factor (DF) dropped below about 10^3 . The progress was also monitored by observing the color of the AgZ bed. The loading distribution on the AgZ bed was then determined by making a vertical scan with a scintillation counter. Eight regions were counted over the 20 cm bed length using an 8 mm slit window in a 2 cm thick lead shield. A similar scan was made after each of the succeeding stages.

Following the loading stage, the AgZ bed temperature was raised to 300°C, and argon or 6% H_2 in helium was passed through the bed to remove excess water from the zeolite. For this operation, the system was closed except for a

(a) Datatest Corporation, Levittown, Pennsylvania.



R - ROTAMETER
 H - PREHEATER FOR AIR SUPPLY
 T - IODINE TRAP, TYPICALLY AgX
 CON. - CONDENSER FOR WATER VAPOR, TEMPERATURE $\sim 5^{\circ}\text{C}$
 GEN. - I_2 GENERATOR
 ABS - ABSORBER FOR I_2 RELEASED DURING DRYING CYCLE.
 SEE TEXT

M - OXYGEN DETECTOR
 C - "CAJON" FITTING FOR GLASS TO METAL JOINT
 P - PRESSURE GAGE
 TC - THERMOCOUPLE
 B - BALL JOINT
 NOX - BULB FOR NO_2 PRODUCTION
 --- HEATED LINE

FIGURE 1. Iodine Loading and Stripping Experimental Apparatus

small bleed stream of argon. The gas stream passed through the first condenser for the first hour or two, and most of the water was removed.

Unfortunately, considerable I_2 was released from the AgZ bed during drying. This came as no surprise, for our previous studies had shown that a large fraction of the iodine loaded beyond about 25-30% theoretical silver utilization is loosely bound in molecular form and easily removed by heating (Scheele and Burger 1980; Scheele and Weimers 1980; Burger and Scheele 1981; Scheele and Burger 1981). In the present experiments, the released I_2 tended to move throughout the system (it was not trapped by PbX), and a portion of it was redistributed back onto the bottom of the AgZ bed.

A secondary problem involved severe corrosion of the stainless steel components, which occurred both during the drying stage and the subsequent stripping stage. During several of the cycles, the lines plugged with what appeared to be a mixture of I_2 and metal iodides. The most severe result of the corrosion, however, was the destruction of the stainless steel bellows in the circulating pump, pump no. 3, which was used in both the drying and stripping stages. The bellows in the pump would typically last for 3-6 runs. In a few of the runs, an additional charcoal or a zeolite trap was inserted in the line at point b to remove iodine from the system.

It should be emphasized that the purpose of this work was to examine the behavior of AgZ under recycle. The remainder of the system was adjusted or modified occasionally to facilitate the operation and does not necessarily represent what would be used in an actual application.

Following the drying operation, hydrogen was passed into the system, replacing the argon, and the temperature of the AgZ bed raised to about 500°C. This treatment removed the iodine, usually as HI. It was difficult to maintain a uniform temperature in the bed, and typically the very top of the bed was 30-50° hotter than the remainder. A small bleed stream, about 100 mL/min of H_2 , was continually added to the system. Before terminating the stripping stage, the circulating H_2 was tested for HI by passing a portion through a fresh AgX bed.

The previous recycle work of Thomas and coworkers (1977, 1978), as well as more recent experiments in our laboratory, have shown that the reduced silver mordenite, Ag^oZ , is operable in the NO_x-H_2O concentration regimes

typical of off-gas streams. Therefore, these variables, as well as temperature and flow rate, were fixed for this study. Details for each stage of the cycle are given in Tables 1 and 2.

TABLE 1: Zeolite^(a) Bed Descriptions

	<u>AgZ</u>	<u>PbX</u>
Bed diameter	5 cm	5 cm
Depth	20 cm	20 cm
Particle Size	10-16 mesh	1.5 mm beads
Mass (dry)	320 g	400 g
Silver content	0.55 mol	--
Lead content	--	0.65 mol

(a) Zeolites obtained from the Ionex Research Corporation, Broomfield, Colorado. The AgZ was 19% Ag by weight (dry).

TABLE 2. Experimental Operating Conditions for AgZ and PbX Beds During Iodine Loading and AgZ Recycle

	<u>Loading</u>		<u>Drying</u>		<u>Stripping</u>	
	<u>AgZ</u>	<u>PbX</u>	<u>AgZ</u>	<u>PbX</u>	<u>AgZ</u>	<u>PbX</u>
Temperature, °C	150±10	X	300	150	460-550	150
Carrier gas	Air	X	Ar or 6% H ₂ in He		H ₂	
Flow rate, L/min	30	X	2-4		24-30	
m/min	15	X	1-2		12-15	
I ₂ conc, µmol/L	10-20	X	Variable		low	
HI conc, µmol/L	0	X	0	0	0	20 (est.)
H ₂ O conc, µmol/L	200-500	X	Variable		Very low	
NO _x conc, %	2	X	0	0	0	0
Run time, hr	4-8	X	8-16		12-24	

X - not in system

RESULTS

In this study, we used two separate beds. The first was loaded, stripped, and reloaded to test the system and check for reproducibility. The second was employed for the long-term recycle study.

The first loading was on unreduced AgZ. The top of the bed loaded to about 160 mg I/g AgZ, and the loading fell off rapidly below section 5 (the 12.5 cm mark as measured from the bed top). Stripping was completed in 20 hrs. The second loading on the reduced Ag^oZ was higher - about 220 mg I/g AgZ at the top sections. Again, the concentrations fell off rapidly in sections 6, 7, and 8. Actual scan data are listed in Tables A.1-A.45 in the Appendix. The apparently low iodine concentration at the top of the bed in this and other runs is an artifact resulting from the counting geometry. The average iodine content for the first loading was 106 mg I/g AgZ zeolite, and for the second, 155 mg I/g AgZ.

New AgZ was then placed in the reaction vessel and the second series of runs started. The first loading was similar to the first on bed 1 and produced a maximum concentration (loading) of about 160 mg I/g AgZ and an average of 110 mg I/g AgZ. The drying cycle for this run employed 6% H₂ in helium at 300°C. About 21% of the iodine was removed during drying.

The 6% H₂-He test in place of argon was performed to eliminate residual NO_x on the AgZ and to determine whether the elemental iodine released during the drying cycle could be converted to HI and trapped by the PbX. Though apparently successful on both counts, we returned to the use of argon in subsequent runs since an inert gas was suggested for the recycle evaluation. We did, in later runs, employ the 6% H₂-He in an effort to reduce the corrosion problems attendant with the circulation of iodine.

After 5 cycles, a noticeable degradation of the bed became manifested in either or both a decreased loading capacity or more commonly a poor I₂ removal with the hydrogen stripping. At the end of the 10th run, following the normal stripping treatment, the total iodine remaining was still 137 mg I/g AgZ. It was reloaded in run 11 and exposed to three separate hydrogen treatments for 23, 21, and 24 hrs, respectively, at about 530°C, which finally reduced the total iodine to 21.4 mg I/g AgZ. The bed was reloaded, and again showed very poor stripping behavior. The temperature was raised to 550-555°C and

restripped. Most of the residual iodine (except that at the top of the bed) was removed. We concluded that the experimental apparatus was inadequate to furnish further information, and the work was terminated.

The runs beyond the initial loading are discussed individually below, and a brief summary is given in Table 3.

Loading 2 averaged 120 mg I/g AgZ with a maximum concentration of about 175. During drying, 18% was removed, and another 80% upon stripping with H₂, leaving 2.4% of the I₂ on the bed. A charcoal trap was placed in the loop in an attempt to trap some of the iodine volatilized as I₂ during the drying stage and the first few minutes of the H₂ stripping. It was largely ineffective; much of the I₂ was deposited on tubing throughout the system.

Loading 3 averaged 104 mg I/g AgZ, and about 4% was removed by drying. A crack developed in the reaction vessel towards the end of the stripping. The

TABLE 3. Summary of Iodine Loading and Stripping

<u>Cycle</u>	<u>Average Cycle Loading mg I/g AgZ</u>	<u>Average Total Loading mg I/g AgZ</u>	<u>Average Total Loading After Stripping mg I/g AgZ</u>
1	110	110	0
2	120	120	3
3	101	104	11
4	84	96	15
5	69	84	60
6	82	142	70
7	125	195	114
8	85	199	140
9	61	201	123
10	47	170	137
11	58	195	21
12	94	116	44

zeolite was transferred in 2 cm segments to a new reaction vessel for completion of the cycle. About 92% of the remaining I_2 was removed by hydrogen stripping at 500°C, leaving about 2.7 g I on the bed. The total iodine on the bed at this point was about 3.6 g I or 11.4 mg I/g AgZ.

It may be noted that whether or not iodine is removed at the drying stage largely depends on the effectiveness of the trapping downstream from the AgZ bed. In a few cases, the removal was aided by leaks, which developed during the heat-up for drying! I_2 not removed from the circulating gas stream was deposited back on the 300°C AgZ bed. In some cases, this was seen as an increased ^{131}I count at the bottom sections of the AgZ bed. I_2 was not trapped by the PbX bed. Even though hydrogen was present, a second release of I_2 occurred when the AgZ bed was heated from 300 to 500°C for the stripping stage.

Loading 4 ran without complication and was completed in 4 hours to a maximum of about 145 mg I/g AgZ and an average of 96. In the drying step, all but about 2% of the released I_2 was trapped back on the AgZ bed. About 95% of the cycle iodine was released by stripping with H_2 , leaving 4 mg/g AgZ of the freshly deposited iodine for a total of about 15 mg I/g AgZ on the bed.

During cycle 5, a crack in the air preheater occurred and caused an interruption in the loading stage. Breakthrough occurred in a total of about 4 hours. During the drying stage, the bellows of the recirculating pump failed due to corrosion, and some iodine was lost from the system. Considerable iodine was also trapped in the condenser, Con-1. The maximum loading was 145 mg I/g AgZ and the average 84 mg I/g AgZ. About 45% of the cycle 5 iodine was removed during drying. During stripping, a new leak developed from corrosion through the 13 mm stainless tubing. After repair, a second hydrogenation step was carried out for a total stripping time of 54 hrs. Stripping removed 35% of the added iodine. At this point, considerable iodine remained on the bed. A total of about 60 mg I/g AgZ or 19 g I appeared to be rather firmly fixed in the zeolite.

Cycle 6 added about 26 g I during loading of about 82 mg I/g AgZ (143 mg I/g AgZ total). The total iodine loading at the top of the bed was quite high at this point, over 200 mg I/g AgZ. Drying removed 15% of the cycle 6 iodine and somewhat leveled the distribution on the bed. Stripping removed an additional 79% and appeared to also remove a portion of the residual iodine from

cycle 5 from bed sections 4 and 5. The total iodine on the bed, at this time, averaged 70 mg I/g AgZ, and about 150 mg I/g AgZ was at the top of the bed.

Cycle 7 was loaded over a 6 hour period, and an average of 195 mg I/g AgZ added to the bed before breakthrough. Note in Table A.21 that the loading at the top of the bed is very high, 336 mg I/g AgZ (225 maximum theoretical on a total silver basis). The 5% of the I₂ removed by drying was deposited in the condensers and in the connecting tubing. Stripping for 28 hours, with temperatures ranging up to 540°C, removed an additional 64%. A second stripping at 500°C left the bed unchanged.

Cycle 8 loaded in about 2.5 hours. It was dried for 14 hours. A small leak was repaired during the 27 hour stripping stage. Considerable reloading and redistribution of the iodine occurred during the drying stage. Actually, the ¹³¹I counting data suggest that some additional iodine may have been picked up from the remainder of the system and deposited on the AgZ. The uncertainty here is about 10% (see Appendix tables). Although nothing unusual occurred during the run, the stripping stage removed much of the iodine from the top of the bed. This action had not been observed before. In spite of this loss, however, the residual iodine was still about 200 mg I/g AgZ at the top of the bed and averaged 140 mg I/g AgZ throughout the bed at the end of the cycle.

Cycle 9 took a nominal 3 hours to load. The loading reached a total iodine maximum of 290 mg I/g AgZ (82 mg I/g AgZ new iodine) and a total iodine average of 201 mg I/g AgZ (60 mg I/g AgZ new iodine). Very little iodine was added to the bottom of the bed at breakthrough. Before drying, the circulating pump had to be repaired again, as the valves and bellows had been destroyed by corrosion. Drying removed 89% of the added iodine. The behavior on stripping was unusual. Iodine was removed from the central portions of the bed, including residual iodine from previous runs, and some was deposited at the top. However, the total iodine loading was not greatly reduced.

This loading was characterized by a pronounced pink color in the upper regions of the bed. Although various pink, red, and purple colors are common in iodine-loaded zeolites, the predominant color in these runs was yellow, with occasional dark orange patches or streaks. Typically, after a drying stage with argon, the bed was uniformly yellow. In contrast, cycle 1, which

was dried with 6% H₂ in helium, was black. After H₂ stripping, the bed was a light to medium gray color.

Although color is not necessarily indicative of iodine content -- it is probably associated with the I₂ interaction with oxygen sites in the zeolite lattices -- bands of color are informative. In these experiments, streaks of color often appeared vertically through the bed, suggesting some degree of channeling. We should mention that marked color changes in zeolites are not unique to iodine sorption. See for example, the paper of Jacobs and Uytterhoeven (1978).

Loading 10 required 2 hours to reach breakthrough. The loading added 15 g I₂, or an average of 47 mg I/g AgZ, giving a total of 170 mg I/g AgZ. The peak total iodine loading again was high, 280 mg I/g AgZ at the top of the bed. The top quarter of the bed was pink, and a broad yellow streak extended through the remainder. Drying with the 6% H₂-He for 16 hours at 300-320°C removed 17% of the added iodine. After drying, the color varied from yellow at the bottom, through orange to pink, and to black at the top. A special charcoal trap placed downstream from the PbX bed picked up very little activity, but considerable iodine-containing liquid collected in the remainder of the system during both drying and stripping. Stripping with the usual 100% H₂ at 500-550°C for 20 hours only removed 53% more, leaving 14 mg I/g AgZ of the added iodine on the bed for a total of 137 mg I/g AgZ.

Loading 11 required 2 hours and placed 18 g or 58 mg I/g AgZ on the bed. The bed was dried overnight with 6% H₂-He at 300°C. Some of the iodine from the circulation loop was picked up and reloaded onto the AgZ bed. The total at this point in time was 210 mg I/g AgZ. After the drying stage, the condensers and the charcoal trap were removed from the system and stripping carried out for 24 hours. During this strip, the temperature was low at the bottom of the bed, ~425°. Considerable black, iodine-containing liquid again collected in the system. Insertion of the condensers into the system removed some of the liquid, but the tubing, valves, and rotometers had to be completely cleaned. The pump bellows had again corroded through, and the pump was replaced.

The system, after sitting idle and closed for 3 days, was dried again with 6% H₂-He, and the stripping continued for 23 hours at a uniform temperature throughout the bed of 520-540°C. A third stripping of 18 hours

was then employed at the same temperature. The bed was counted after each treatment.

The first 24 hour strip removed 93% of the iodine. This was the first really efficient stripping run since early in the tests. At the end of the third strip, the total iodine loading was down to 21 mg I/g AgZ, most of which was at the bottom of the bed. The very bottom of the bed was a bright orange color at the end of the run.

Cycle 12 loaded normally, putting about 94 mg I/g AgZ on the bed with a maximum of 160 mg I/g AgZ. The total iodine was 116 mg I/g AgZ. The drying stage was delayed due to pump failure (the bellows was again destroyed). Drying was finally accomplished by using argon from a cylinder and releasing it downstream from the PbX bed through a secondary AgX trap. A flow of 4 L/min was used for about 20 hours. The drying temperature was slightly higher than normal, about 330°C. This removed about 16% of the iodine, which was rather uniformly deposited at valves in the main line, in Con-1 and its receiver, and at the very top of the PbX bed.

For stripping, the temperature was maintained at 510°C or slightly below. No iodine was removed in 24 hours. An additional strip was tried, of 64 hours at the same temperature. About 47% of the iodine was stripped. A third stripping was added, of 48 hours, which removed a small amount. The net loading at the end of the final 500°C strip was 72 mg I/g AgZ, with regions at the top of the bed as high as 140 mg I/g AgZ. A final strip was then added, of 18 hrs at a temperature of 550-555°C. This removed 17% of the cycle 12 iodine, primarily from the upper part of the bed, leaving an average cycle iodine loading of 32 mg I/g AgZ (44 mg I/g AgZ total).

DISCUSSION

Some comment on the nature of zeolites is necessary to appreciate the observations of this report. Mordenite is a high-silica zeolite of nominal composition $\text{Na}_2\text{O} \cdot \text{Al}_2\text{O}_3 \cdot 10 \text{SiO}_2 \cdot 6 \text{H}_2\text{O}$.^(a) Figure 2 presents a stereo view of its structure. There are two sets of channels. The main ones, $6.7 \times 7.0 \text{ \AA}$, are linked in the same plane by small pockets having apertures of about 2.8 \AA . Thus, only for small molecules is the channel system 2-dimensional. I_2 is $\sim 5.3 \text{ \AA}$ along its longitudinal axis. Although blocking of the channels is common in natural mordenites as a result of impurities or crystal faults, this does not appear to be a problem with the synthetic material Zeolon®. Of the 8 sodium atoms of the unit cell, 4 are in small cavities and 4 randomly situated in the large channels. All are apparently replaceable with silver ions; however, they are obviously not equally accessible.

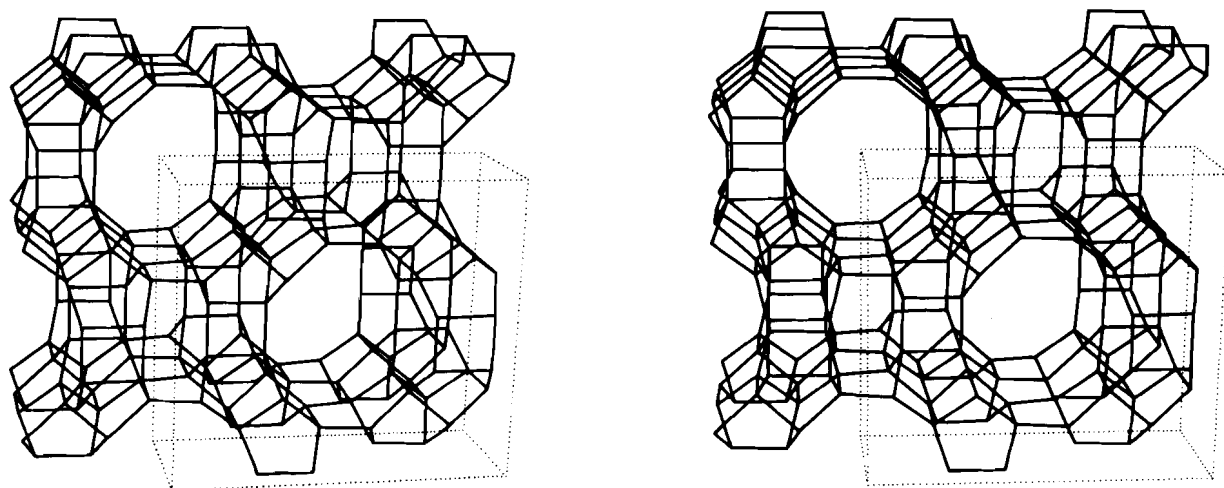


FIGURE 2. Stereo View of Sodium Mordenite, Reprinted with Permission from Meier and Olson (1971). Copyright 1971 American Chemical Society.

(a) Breck (1974) gives a comprehensive survey of zeolite structures.
® Trademark of Norton Chemical Process Products Division, Akron, Ohio.

X-ray structures of several cation-exchanged natural mordenites have been determined by Pluth and coworkers. See, for example, Schlenker, Pluth and Smith (1979). Powder patterns of several silver-substituted zeolites, including silver mordenite, were obtained by Vance and Agrawal (1982). However, no single crystal work has been reported, and the locations of the silver atoms are not certain. The information on mordenites is less well developed than for many other zeolites.

In this study, we have used Zeolon® exclusively. The silver-exchanged material was prepared by Ionex Corporation and had a typical silver content of 19% (dry basis).

Three other comments are necessary. Random assemblies of water molecules in the zeolite cavities may act as micro solutions. Thus, solution phase reactions are possible, such as hydrolysis to form Ag_2O and hydrogen mordenite.

The second comment concerns the reduction of the silver mordenite by hydrogen, which occurs in the stripping stage. The reduced silver atoms tend to form aggregates of considerable size, up to a micrometer in diameter. The extent of the migration of reduced-metal atoms in zeolites and the size of the aggregates or crystallites formed depend on the temperature and on the extent of hydration at the time of reduction. Low temperature and low water content favor the formation of smaller particles (Minachev and Isakov 1976). Figure 3 shows a 1000x magnification of a polished section of iodine-loaded Ag°Z . Scanning electron microscopy, coupled with x-ray fluorescence, indicates that the white particles contain only silver and iodine. Similar scans of unloaded Ag°Z show silver metal particles which are the precursors of the AgI particles (Scheele et al. 1980).

Thirdly, stages of the recycle process, subsequent to the reduction, subject the silver particles to $\text{H}_2\text{O} + \text{O}_2$ followed by $\text{H}_2\text{O} + \text{NO}_x + \text{I}_2$ and may redistribute some of the silver. However, the presence of NO is expected to keep the silver in reduced form during the loading stage (Thomas, Staples and Murphy 1978). Thus, silver aggregates are expected to be the normal occurrence, and they probably increase with each cycle. This has not been confirmed, however. The important point is that the chemistry of this loading, drying, stripping cycle is very complex and is probably not always

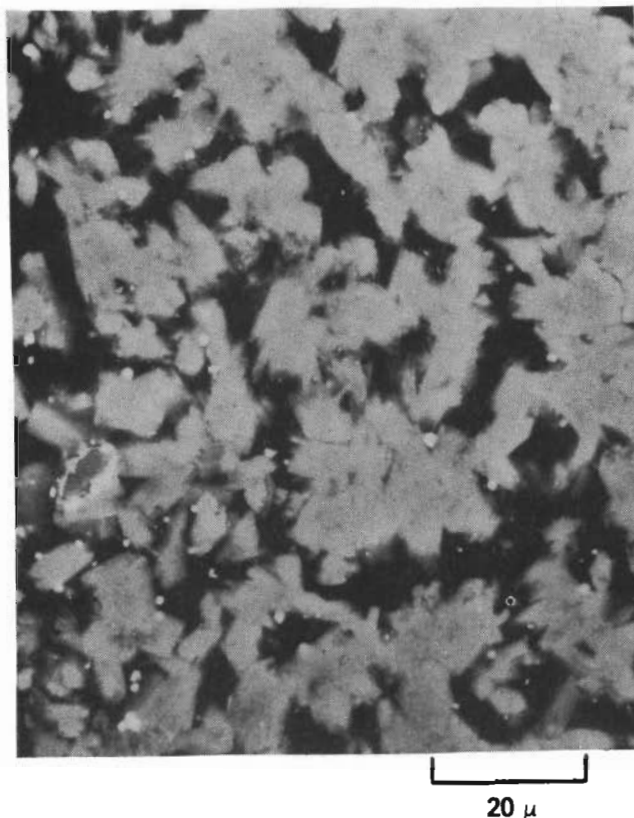


FIGURE 3. Scanning Electron Micrograph of 100 mg I/g Ag°Z

reproducible under the conditions of the experiment. Unfortunately, the program did not permit us to examine the details of the chemical mechanisms.

The test result data confirm previous work that silver mordenite can indeed be recycled. There appears to be no major degradation of Ag°Z with respect to iodine pickup. However, there is evidence that stripping becomes more difficult as early as the 5th cycle. For the iodine held as AgI, the stripping is thermodynamically unfavorable, and the calculated HI partial pressures for the reaction $\text{AgI} + 1/2 \text{H}_2 \rightarrow \text{Ag}^\circ + \text{HI}$, based on data from Barin and Knacke (1973), are 9×10^{-4} atm at 500° and 3.2×10^{-3} atm at 600°C. The present experiments suggest that a temperature of 550°C or greater is desirable, in agreement with these calculations. However, it has been shown that AgZ loses its zeolitic structure at 700°C (Vance and Agrawal 1982). In the presence of $\text{H}_2\text{O} + \text{NO}_2$, the maximum safe temperature may be even lower. It should also be noted that the volatility of silver iodide becomes appreciable above about 600°C (Scheele and Burger 1980). Thus, a fairly long reduction time at a lower temperature is probably necessary.

Inspection of Tables A.1-A.45 indicates that the transfer zone is of the order of 10 cm under the conditions of the experiment. It would appear that a 15 cm bed could be loaded to a high capacity without breakthrough. Some channeling was observed with the 10-16 mesh material used here. Previous work at our laboratory has shown that the transfer zone is much shorter for 20-40 mesh zeolite and also at lower face velocities with 10-16 mesh AgZ.

As was noted earlier, our previous work had shown that only about 25-30% of the stoichiometric-loaded iodine on AgZ is chemically bound, e.g., as AgI and stable to heating. The remainder is molecularly bound and volatilizes as I₂, starting at about 250-300°C. This has been confirmed by Vance and Agrawal (1982). At the temperature of the reduction, 500-550°C, much of the iodine is removed whether or not the hydrogen is present. A realistic recycle design would have to accommodate this fact rather than provide only for trapping HI.

Jubin (1980) had good success removing I₂ from AgZ using 4.5% H₂ in argon. He found, however, that the zeolite was degraded with respect to further iodine loading.

Aside from the substitution of 6% H₂-He for argon in 3 runs, the drying stage was not studied. With virtually any flowing gas at 300°C, zeolites can usually be dried in a few minutes to a small percentage of their saturated water content. The NO_x may add some complications. However, the overnight drying period was more of a convenience than a necessity. Although, as noted earlier, the amount of water in the zeolitic pores may influence the physical behavior of the silver during reduction, a separate drying cycle may actually be unnecessary.

Corrosion was severe during these experiments; the HI-I₂-H₂O system is incompatible with stainless steel. Thus, Monel® or other construction materials need to be investigated.

In this study, we evaluated the effects of hydrogen recycle of AgZ on I₂ capture and delayed study on the effect of AgZ recycle on organic iodide capture. However, other work has shown that hydrogen-reduced AgZ is an effective trap for methyl iodide (Scheele and Wiemers 1980; Scheele, Matsuzaki and Burger 1981). Recycled AgZ should behave similarly.

In summary, AgZ can be recycled, but the cycle, as tested here, would have to be modified to trap I_2 -- a major release product -- before trapping the HI in PbX. An alternative scheme might trap both in an aqueous system. It may be necessary to raise the stripping temperature to 550-600°C. If it is, indeed, necessary to reuse the AgZ, an alternative process would be: 1) to load AgZ to maximum capacity (this can be greater than theoretical), 2) to drive off the 60-80% I_2 not strongly bound with air or nitrogen at 400-600°C, and 3) to reload with iodine. Series operation of beds should guarantee the required decontamination factor. Occasionally, if desired, a bed could be removed to a separate facility after the 400-600°C treatment and stripped with pure or dilute H_2 at 550-600°C.

•

•

•

•

•

•

•

•

ACKNOWLEDGEMENTS

We would like to thank R. J. Elovich, C. L. Matsuzaki and L. A. Rogers for their help in the laboratory. We would also like to thank L. D. Maki and D. L. Futch for typing the report and S. F. Liebetrau for her editorial advice.

✓

✓

✓

•

•

•

•

•

REFERENCES

- Barin, I., and O. Knacke. 1973. Thermochemical Properties of Inorganic Substances. Springer-Verlag, Berlin, Germany.
- Breck, D. W. 1974. Zeolite Molecular Sieves. Wiley-Interscience, New York.
- Burger, L. L. and R. D. Scheele. 1981. "Iodine Fixation Studies at the Pacific Northwest Laboratory." Paper Presented at the Specialists Meeting on Radioiodine Management, September 25, 1981, Brussels, Belgium. PNL-SA-9829, Pacific Northwest Laboratory, Richland, Washington.
- Burger, L. L., R. D. Scheele and K. D. Wiemers. 1981. Selection of a Form for Fixation of Iodine-129. PNL-4045, Pacific Northwest Laboratory, Richland, Washington.
- Jacobs, P. A., J. B. Uytterhoeven and H. K. Beyer. 1978. "Some Unusual Properties of Activated and Reduced AgNaA Zeolites." J. Chem. Soc., Faraday Trans. I., 75: 56.
- Jubin, R. T. 1980. Organic Iodine Removal from Simulated Dissolver Off-Gas Streams Using Silver-Exchanged Mordenite. Presented at the 16th DOE Air Cleaning Conference, San Diego, California.
- Meier, W. T., and D. H. Olson. 1971. "Zeolite Frameworks." In Molecular Sieve Zeolites, R. F. Gould, ed. Advances in Chemistry Series 101, ACS, Washington, D. C.
- Minachev, K. H., and Y. I. Isakov. 1976. "Catalytic Properties of Metal-Containing Zeolites." In Zeolite Chemistry and Catalysis, Ed. J. A. Rabo, pp. 552-611. ACS Monograph No. 171. American Chemical Society, Washington, D. C.
- Murphy, L. P., B. A. Staples and T. R. Thomas. 1977. The Development of Ag⁰Z for Bulk ¹²⁹I Removal from Nuclear Fuel Reprocessing Plants and PbX for ¹²⁹I Storage. ICP-1135, Allied Chemical Corporation, Idaho Falls, Idaho.
- Scheele, R. D., and L. L. Burger. 1981. "Characterization Studies of Iodine Loaded Silver Zeolites." PNL-SA-9510. Paper presented at the 182nd National Meeting of the American Chemical Society, August 23-28, 1981, New York.
- Scheele, R. D., and L. L. Burger. 1980. "Iodine-129 Fixation," In Nuclear Waste Management Quarterly Progress Report, April Through June 1980. A. M. Platt and J. A. Powell, Eds. PNL-3000-6, Pacific Northwest Laboratory, Richland, Washington.
- Scheele, R. D., C. L. Matsuzaki and L. L. Burger. 1981. "Iodine-129 Fixation." In Nuclear Waste Management Quarterly Progress Report October through December 1981, compiled by T. D. Chikalla and J. A. Powell. PNL-3000-10, Pacific Northwest Laboratory, Richland, Washington.

- Scheele, R. D., and K. D. Wiemers. 1980. "Iodine-129 Fixation." In Nuclear Waste Management Quarterly Progress Report, January Through March 1980. A. M. Platt and J. A. Powell, eds. PNL-3000-5, Pacific Northwest Laboratory, Richland, Washington.
- Scheele, R. D., et al. 1980. "Iodine-129 Fixation." In Nuclear Waste Management Quarterly Progress Report, July Through September 1980. T. D. Chikalla and J. A. Powell, eds. PNL-3000-7, Pacific Northwest Laboratory, Richland, Washington.
- Schlenker, J. L., J. J. Pluth and J. V. Smith. 1979. "Positions of Cations and Molecules in Zeolites with the Mordenite-Type Framework X Dehydrated Calcium Hydrogen Mordenite." Mat. Res. Bull. 14(8):961-966.
- Thomas, T. R., et al. 1977. Airborne Elemental Iodine Loading Capacities of Metal Zeolites and a Method for Recycling Silver Zeolite. ICP-1119, Allied Chemicals Corporation, Idaho Falls, Idaho.
- Thomas, T. R., B. A. Staples and L. P. Murphy. 1978. The Development of Ag⁰Z for Bulk ¹²⁹I Removal from Nuclear Fuel Reprocessing Plants and PbX for ¹²⁹I Storage. Presented at the 15th DOE Nuclear Air Cleaning Conference, August 1978. Boston, Massachusetts. CONF 780819, p. 34.
- Vance, E. R., and D. K. Agrawal. 1982. "X-ray Studies of Iodine Sorption in Some Silver Zeolites." J. Mat. Sci. 17: 1889-1894.

APPENDIX

TABLES OF IODINE-LOADING CHARACTERISTICS FOR EACH CYCLE

•

•

•

•

•

•

•

•

TABLE A.1 Iodine-Loading Characteristics for AgZ Bed 1, Cycle 1, Loading Stage

<u>AgZ Bed Segment</u>	<u>Cycle Loading, g I</u>	<u>Cycle Loading, mg I/g AgZ</u>
1	6.0	148
2	6.4	160
3	6.2	154
4	5.7	140
5	4.8	118
6	3.1	77
7	1.4	34
8	0.6	14
Total	34.2	
Average		106

TABLE A.2. Iodine-Loading Characteristics for AgZ Bed 1, Cycle 1, Drying Stage

<u>AgZ Bed Segment</u>	<u>Cycle Loading, g I</u>	<u>Cycle Loading, mg I/g AgZ</u>
1	4.3	106
2	4.7	116
3	4.5	112
4	4.3	106
5	4.3	106
6	4.3	107
7	4.5	112
8	3.3	82
Total	34.2	
Average		106

100% of cycle iodine remains.

TABLE A.3. Iodine-Loading Characteristics for AgZ Bed 1, Cycle 2, Loading Stage

<u>AgZ Bed Segment</u>	<u>Cycle Loading, g I</u>	<u>Cycle Loading, mg I/g AgZ</u>
1	6.3	157
2	8.4	202
3	8.8	217
4	7.9	196
5	8.7	216
6	4.8	118
7	2.5	63
8	2.2	54
Total	49.7	
Average		155

TABLE A.4. Iodine-Loading Characteristics for AgZ Bed 2, Cycle 1, Loading Stage

<u>AgZ Bed Segment</u>	<u>Cycle Loading, g I</u>	<u>Cycle Loading, mg I/g AgZ</u>
1	5.8	136
2	6.5	152
3	6.3	147
4	6.0	142
5	5.4	126
6	4.2	99
7	2.6	61
8	0.7	17
Total	37.6	
Average		110

TABLE A.5. Iodine-Loading Characteristics for AgZ Bed 2, Cycle 1, Drying Stage

<u>AgZ Bed Segment</u>	<u>Cycle Loading, g I</u>	<u>Cycle Loading, mg I/g AgZ</u>
1	5.1	118
2	5.2	122
3	5.1	120
4	4.7	110
5	4.2	99
6	3.2	76
7	1.8	43
8	0.33	8
Total	29.8	
Average		87

79.2% of cycle iodine remains.

TABLE A.6. Iodine-Loading Characteristics for AgZ Bed 2, Cycle 2, Loading Stage

<u>AgZ Bed Segment</u>	<u>Cycle Loading, g I</u>	<u>Cycle Loading, mg I/g AgZ</u>
1	6.3	157
2	7.0	175
3	6.8	169
4	6.4	160
5	5.2	131
6	4.0	100
7	2.2	55
8	0.71	18
Total	38.5	
Average		120

TABLE A.7. Iodine-Loading Characteristics for AgZ Bed 2, Cycle 2, Drying Stage

<u>AgZ Bed Segment</u>	<u>Cycle Loading, g I</u>	<u>Cycle Loading, mg I/g AgZ</u>
1	5.4	136
2	5.9	148
3	5.4	136
4	4.8	119
5	4.1	102
6	3.3	83
7	1.8	46
8	0.61	15
Total	31.4	
Average		98

81.5% of cycle iodine remains.

TABLE A.8. Iodine-Loading Characteristics for
AgZ Bed 2, Cycle 2, Stripping Stage

<u>AgZ Bed Segment</u>	<u>Cycle Loading, g I</u>	<u>Cycle Loading, mg I/g AgZ</u>
1	0.05	1.3
2	0.01	0.3
3	0.08	2.0
4	0.10	2.5
5	0.10	2.5
6	0.08	1.9
7	0.18	4.4
8	0.35	8.6
Total	0.94	
Average		2.9

2.4% of cycle iodine remains.

TABLE A.9. Iodine-Loading Characteristics for AgZ Bed 2, Cycle 3, Loading Stage

<u>AgZ Bed Segment</u>	<u>Cycle Loading, g I</u>	<u>Cycle Loading, mg I/g AgZ</u>	<u>Total Loading mg I/g AgZ</u>
1	6.1	152	153
2	7.0	175	175
3	6.8	169	171
4	5.9	148	150
5	4.0	101	104
6	1.8	45	47
7	0.6	15	20
8	0.0	0.0	3
Total	32.2		
Average		101	104

TABLE A.10. Iodine-Loading Characteristics for AgZ Bed 2, Cycle 3, Drying Stage

<u>AgZ Bed Segment</u>	<u>Cycle Loading, g I</u>	<u>Cycle Loading, mg I/g AgZ</u>	<u>Total Loading mg I/g AgZ</u>
1	6.9	172	174
2	6.4	160	160
3	6.0	150	152
4	5.1	128	130
5	3.6	90	92
6	1.9	48	51
7	0.73	18	23
8	0.20	5	14
Total	30.8		
Average		96	99

95.7% of cycle iodine remains.

TABLE A.11. Iodine-Loading Characteristics for
AgZ Bed 2, Cycle 3, Stripping Stage

<u>AgZ Bed Segment</u>	<u>Cycle Loading, g I</u>	<u>Cycle Loading, mg I/g AgZ</u>	<u>Total Loading, mg I/g AgZ</u>
1	0.39	10	11
2	0.34	8	9
3	0.29	7	9
4	0.40	9	12
5	0.34	8	11
6	0.36	9	11
7	0.08	2	6
8	0.52	13	22
Total	2.71		
Average		8	11

8.4% of cycle iodine remains.

TABLE A.12. Iodine-Loading Characteristics for AgZ Bed 2, Cycle 4, Loading Stage

<u>AgZ Bed Segment</u>	<u>Cycle Loading, g I</u>	<u>Cycle Loading, mg I/g AgZ</u>	<u>Total Loading, mg I/g AgZ</u>
1	4.7	116	128
2	5.4	136	145
3	4.8	119	128
4	4.3	107	119
5	3.6	91	102
6	2.4	61	72
7	1.4	34	40
8	0.44	11	22
Total	27.0		
Average		84	96

TABLE A.13. Iodine-Loading Characteristics for AgZ Bed 2, Cycle 4, Drying Stage

<u>AgZ Bed Segment</u>	<u>Cycle Loading, g I</u>	<u>Cycle Loading, mg I/g AgZ</u>	<u>Total Loading, mg I/g AgZ</u>
1	3.8	96	97
2	5.0	125	134
3	4.6	115	124
4	4.3	106	118
5	3.8	95	106
6	2.7	68	79
7	1.5	38	44
8	0.46	12	32
Total	26.4		
Average		82	94

97.8% of cycle iodine remains.

TABLE A.14. Iodine-Loading Characteristics for
AgZ Bed 2, Cycle 4, Stripping Stage

<u>AgZ Bed Segment</u>	<u>Cycle Loading, g I</u>	<u>Cycle Loading, mg I/g AgZ</u>	<u>Total Loading, mg I/g AgZ</u>
1	0.07	2	13
2	0.05	1	10
3	0.11	3	12
4	0.11	3	15
5	0.16	4	15
6	0.17	4	15
7	0.23	6	12
8	0.33	8	30
Total	1.23		
Average		15	

4.7% of cycle iodine remains.

TABLE A.15. Iodine-Loading Characteristics for AgZ Bed 2, Cycle 5, Loading Stage

<u>AgZ Bed Segment</u>	<u>Cycle Loading, g I</u>	<u>Cycle Loading, mg I/g AgZ</u>	<u>Total Loading, mg I/g AgZ</u>
1	2.9	72	84
2	5.3	133	143
3	5.0	124	136
4	3.9	97	112
5	2.2	56	71
6	1.2	29	44
7	0.65	16	28
8	0.25	6	36
Total	22.0		
Average		69	84

TABLE A.16. Iodine-Loading Characteristics for AgZ Bed 2, Cycle 5, Drying Stage

<u>AgZ Bed Segment</u>	<u>Cycle Loading, g I</u>	<u>Cycle Loading, mg I/g AgZ</u>	<u>Total Loading mg I/g AgZ</u>
1	0.93	23	36
2	3.1	78	87
3	3.1	78	90
4	2.6	65	80
5	1.6	39	54
6	0.61	15	30
7	0.18	4	17
8	0.07	2	32
Total	12.2		
Average		38	53

55.1% of cycle loading remains.

TABLE A.17. Iodine-Loading Characteristics for
AgZ Bed 2, Cycle 5, Stripping Stage

<u>AgZ Bed Segment</u>	<u>Cycle Loading, g I</u>	<u>Cycle Loading, mg I/g AgZ</u>	<u>Total Loading, mg I/g AgZ</u>
1	2.5	63	76
2	3.6	90	100
3	3.6	89	101
4	2.3	57	72
5	0.66	16	31
6	0.15	4	19
7	0.14	4	16
8	0.56	14	44
Total	14.2		
Average		44	60

64.5% of cycle iodine remains.

TABLE A.18. Iodine-Loading Characteristics for AgZ Bed 2, Cycle 6, Loading Stage

<u>AgZ Bed Segment</u>	<u>Cycle Loading, g I</u>	<u>Cycle Loading, mg I/g AgZ</u>	<u>Total Loading, mg I/g AgZ</u>
1	3.2	79	155
2	4.4	111	211
3	4.7	117	218
4	4.8	120	192
5	4.4	111	142
6	2.5	63	82
7	1.6	40	56
8	0.69	17	61
Total	26.4		
Average		82	142

TABLE A.19. Iodine-Loading Characteristics for AgZ Bed 2, Cycle 6, Drying Stage

<u>AgZ Bed Segment</u>	<u>Cycle Loading, g I</u>	<u>Cycle Loading, mg I/g AgZ</u>	<u>Total Loading, mg I/g AgZ</u>
1	1.8	45	121
2	2.7	66	166
3	2.6	64	165
4	7.7	192	264
5	3.6	90	121
6	2.1	54	72
7	1.4	35	50
8	0.45	11	55
Total	22.3		
Average		70	129

84.5% of cycle iodine remains.

TABLE A.20. Iodine-Loading Characteristics for
AgZ Bed 2, Cycle 6, Stripping Stage

<u>AgZ Bed Segment</u>	<u>Cycle Loading, g I</u>	<u>Cycle Loading, mg I/g AgZ</u>	<u>Total Loading, mg I/g AgZ</u>
1	2.7	66	142
2	2.3	58	158
3	0.22	5	106
4	0	0	34
5	0	0	31
6	0.13	3	22
7	0.04	1	17
8	0.10	2	46
Total	5.49		
Average		17	70

20.7% of cycle iodine remains.

TABLE A.21. Iodine-Loading Characteristics for AgZ Bed 2, Cycle 7, Loading Stage

<u>AgZ Bed Segment</u>	<u>Cycle Loading, g I</u>	<u>Cycle Loading, mg I/g AgZ</u>	<u>Total Loading, mg I/g AgZ</u>
1	4.5	113	255
2	7.1	178	336
3	8.3	207	313
4	8.1	202	236
5	5.8	144	175
6	3.2	80	102
7	2.2	54	70
8	0.98	24	71
Total	40.0		
Average		125	195

TABLE A.22. Iodine-Loading Characteristics for AgZ Bed 2, Cycle 7, Drying Stage

<u>AgZ Bed Segment</u>	<u>Cycle Loading, g I</u>	<u>Cycle Loading, mg I/g AgZ</u>	<u>Total Loading, mg I/g AgZ</u>
1	4.3	107	249
2	6.1	151	309
3	7.3	182	288
4	7.0	175	209
5	6.4	159	190
6	3.7	93	115
7	2.3	57	74
8	1.0	25	71
Total	38.0		
Average		119	189

95.0% of cycle iodine remains.

TABLE A.23. Iodine-Loading Characteristics for AgZ Bed 2, Cycle 7, Stripping Stage #1

<u>AgZ Bed Segment</u>	<u>Cycle Loading, g I</u>	<u>Cycle Loading, mg I/g AgZ</u>	<u>Total Loading mg I/g AgZ</u>
1	1.4	36	178
2	2.0	50	208
3	3.0	74	180
4	3.0	75	110
5	2.4	61	93
6	1.1	26	48
7	0.71	18	34
8	0.63	16	62
Total	14.3		
Average		45	114

35.7% of cycle iodine remains.

TABLE A.24. Iodine-Loading Characteristics for AgZ Bed 2, Cycle 7, Stripping Stage #2

<u>AgZ Bed Segment</u>	<u>Cycle Loading, g I</u>	<u>Cycle Loading, mg I/g AgZ</u>	<u>Total Loading mg I/g AgZ</u>
1	1.8	45	187
2	2.1	53	211
3	2.9	72	178
4	2.9	72	106
5	2.3	57	88
6	0.88	22	44
7	0.65	16	33
8	0.76	19	15
Total	14.3		
Average		45	114

37.9% of cycle iodine remains.

TABLE A.25. Iodine-Loading Characteristics for AgZ Bed 2, Cycle 8, Loading Stage

<u>AgZ Bed Segment</u>	<u>Cycle Loading, g I</u>	<u>Cycle Loading, mg I/g AgZ</u>	<u>Total Loading mg I/g AgZ</u>
1	3.8	95	282
2	5.3	132	343
3	4.6	114	292
4	3.9	97	203
5	3.3	83	172
6	2.8	70	114
7	2.4	61	94
8	0.99	25	90
Total	27.1		
Average		85	199

TABLE A.26. Iodine-Loading Characteristics for AgZ Bed 2, Cycle 8, Drying Stage

<u>AgZ Bed Segment</u>	<u>Cycle Loading, g I</u>	<u>Cycle Loading, mg I/g AgZ</u>	<u>Total Loading mg I/g AgZ</u>
1	2.7	68	265
2	3.8	95	320
3	3.8	94	286
4	3.6	89	208
5	3.9	97	200
6	4.3	107	167
7	3.6	89	135
8	1.6	40	111
Total	27.1		
Average		85	212

115% of cycle iodine remains.
Assumed no iodine loss for calculations.

TABLE A.27. Iodine-Loading Characteristics for
AgZ Bed 2, Cycle 8, Stripping Stage

<u>AgZ Bed Segment</u>	<u>Cycle Loading, g I</u>	<u>Cycle Loading, mg I/g AgZ</u>	<u>Total Loading mg I/g AgZ</u>
1	0.00	0.0	144
2	0.00	0.0	211
3	0.52	13	191
4	0.53	13	119
5	1.5	36	125
6	2.6	65	109
7	2.2	54	87
8	1.0	26	91
Total	8.35		
Average		26	140

30.6% of cycle iodine remains.

TABLE A.28. Iodine-Loading Characteristics for
Bed 2, Cycle 9, Loading Stage

<u>AgZ Bed Segment</u>	<u>Cycle Loading, g I</u>	<u>Cycle Loading, mg I/g AgZ</u>	<u>Total Loading mg I/g AgZ</u>
1	5.7	143	287
2	3.3	82	293
3	3.3	82	273
4	3.2	79	198
5	2.1	52	177
6	1.2	29	138
7	0.71	18	105
8	0.00	0.0	74
Total	19.4		
Average		61	201

TABLE A.29. Iodine-Loading Characteristics for
AgZ Bed 2, Cycle 9, Drying Stage

<u>AgZ Bed Segment</u>	<u>Cycle Loading, g I</u>	<u>Cycle Loading, mg I/g AgZ</u>	<u>Total Loading mg I/g AgZ</u>
1	0.97	24	168
2	0.26	6	217
3	0.00	0.0	186
4	0.54	13	132
5	0.19	5	130
6	0.00	0.0	103
7	0.25	6	94
8	0.00	0.0	67
Total	2.2		
Average		7	151

11.4% of cycle iodine remains.

TABLE A.30. Iodine-Loading Characteristics for
AgZ Bed 2, Cycle 9, Stripping Stage

<u>AgZ Bed Segment</u>	<u>Cycle Loading, g I</u>	<u>Cycle Loading, mg I/g AgZ</u>	<u>Total Loading mg I/g AgZ</u>
1	1.8	45	189
2	0.00	0.0	208
3	0.00	0.0	164
4	0.00	0.0	101
5	0.00	0.0	90
6	0.00	0.0	78
7	0.00	0.0	76
8	0.42	11	77
Total	2.22		
Average		7	123

13.8% of cycle iodine remains.

TABLE A.31. Iodine-Loading Characteristics for AgZ Bed 2, Cycle 10, Loading Stage

<u>AgZ Bed Segment</u>	<u>Cycle Loading, g I</u>	<u>Cycle Loading, mg I/g AgZ</u>	<u>Total Loading mg I/g AgZ</u>
1	2.4	59	248
2	3.0	75	283
3	3.3	83	247
4	2.8	70	171
5	2.0	51	141
6	1.1	27	105
7	0.5	12	88
8	0.04	1	78
Total	15.2		
Average		47	170

TABLE A.32. Iodine-Loading Characteristics for AgZ Bed 2, Cycle 10, Drying Stage

<u>AgZ Bed Segment</u>	<u>Cycle Loading, g I</u>	<u>Cycle Loading, mg I/g AgZ</u>	<u>Total Loading mg I/g AgZ</u>
1	1.1	26	215
2	2.3	57	265
3	2.6	65	229
4	2.6	64	169
5	2.2	55	145
6	1.2	31	109
7	0.68	17	92
8	0.047	1	79
Total	12.6		
Average		40	162

83.4% of cycle iodine remains.

TABLE A.33. Iodine-Loading Characteristics for
AgZ Bed 2, Cycle 10, Stripping Stage

<u>AgZ Bed Segment</u>	<u>Cycle Loading, g I</u>	<u>Cycle Loading, mg I/g AgZ</u>	<u>Total Loading mg I/g AgZ</u>
1	1.2	31	220
2	1.7	42	250
3	1.1	27	191
4	0.51	13	114
5	0.080	2	92
6	0.00	0.0	55
7	0.00	0.0	46
8	0.00	0.0	56
Total	4.6		
Average		14	137

30.4% of cycle iodine remains.

TABLE A.34. Iodine Loading Characteristics for AgZ Bed 2, Cycle 11, Loading Stage

<u>AgZ Bed Segment</u>	<u>Cycle Loading, g I</u>	<u>Cycle Loading, mg I/g AgZ</u>	<u>Total Loading mg I/g AgZ</u>
1	1.3	33	253
2	2.8	70	320
3	3.8	95	286
4	4.1	103	217
5	3.1	78	170
6	1.8	46	101
7	1.2	30	77
8	0.29	7	61
Total	18.5		
Average		58	195

TABLE A.35. Iodine Loading Characteristics for AgZ Bed 2, Cycle 11, Drying Stage #1

<u>AgZ Bed Segment</u>	<u>Cycle Loading, g I</u>	<u>Cycle Loading, mg I/g AgZ</u>	<u>Total Loading mg I/g AgZ</u>
1	1.5	38	268
2	2.2	55	319
3	3.1	77	288
4	3.4	85	221
5	3.4	84	198
6	2.7	67	139
7	1.6	41	98
8	0.66	17	77
Total	18.5		
Average		58	210

TABLE A.36. Iodine Loading Characteristics for
AgZ Bed 2, Cycle 11, Stripping Stage #1

<u>AgZ Bed Segment</u>	<u>Cycle Loading, g I</u>	<u>Cycle Loading, mg I/g AgZ</u>	<u>Total Loading mg I/g AgZ</u>
1	0.00	0.0	11
2	0.00	0.0	66
3	0.00	0.0	90
4	0.00	0.0	73
5	0.00	0.0	87
6	0.46	12	67
7	0.57	14	60
8	0.32	8	64
Total	1.35		
Average		34	65

7.35% of cycle iodine remains.

TABLE A.37. Iodine Loading Characteristics for
AgZ Bed 2, Cycle 11, Drying Stage #2

<u>AgZ Bed Segment</u>	<u>Cycle Loading, g I</u>	<u>Cycle Loading, mg I/g AgZ</u>	<u>Total Loading mg I/g AgZ</u>
1	0.00	0.0	10
2	0.00	0.0	14
3	0.00	0.0	20
4	0.00	0.0	16
5	0.00	0.0	39
6	0.00	0.0	50
7	0.00	0.0	44
8	0.42	11	67
Total	0.42		
Average		1	32

2.3% of cycle iodine remains.

TABLE A.38. Iodine Loading Characteristics for
AgZ Bed 2, Cycle 11, Stripping Stage #2

<u>AgZ Bed Segment</u>	<u>Cycle Loading, g I</u>	<u>Cycle Loading, mg I/g AgZ</u>	<u>Total Loading mg I/g AgZ</u>
1	0.00	0.0	8
2	0.00	0.0	10
3	0.00	0.0	9
4	0.00	0.0	7
5	0.00	0.0	13
6	0.00	0.0	25
7	0.061	2	45
8	0.64	16	72
Total	0.70		
Average		2	24

3.8% of cycle iodine remains.

TABLE A.39. Iodine Loading Characteristics for
AgZ Bed 2, Cycle 11, Stripping Stage #3

<u>AgZ Bed Segment</u>	<u>Cycle Loading, g I</u>	<u>Cycle Loading, mg I/g AgZ</u>	<u>Total Loading mg I/g AgZ</u>
1	0.013	0.3	8
2	0.010	0.2	10
3	0.00	0.0	9
4	0.00	0.0	6
5	0.00	0.0	11
6	0.00	0.0	21
7	0.15	4	48
8	0.54	13	70
Total	0.70		
Average		2	21

3.8% of cycle iodine remains.

TABLE A.40. Iodine Loading Characteristics for AgZ Bed 2, Cycle 12, Loading Stage

<u>AgZ Bed Segment</u>	<u>Cycle Loading, g I</u>	<u>Cycle Loading, mg I/g AgZ</u>	<u>Total Loading mg I/g AgZ</u>
1	4.8	120	128
2	5.8	146	156
3	6.5	162	171
4	5.7	142	148
5	4.1	102	113
6	2.1	53	74
7	0.77	19	67
8	0.23	6	75
Total	30.0		
Average		94	116

TABLE A.41. Iodine Loading Characteristics for AgZ Bed 2, Cycle 12, Drying Stage

<u>AgZ Bed Segment</u>	<u>Cycle Loading, g I</u>	<u>Cycle Loading, mg I/g AgZ</u>	<u>Total Loading mg I/g AgZ</u>
1	3.7	92	101
2	5.2	131	141
3	5.8	145	154
4	4.7	118	124
5	3.5	88	100
6	1.6	41	62
7	0.64	16	64
8	0.014	0.4	70
Total	25.3		
Average		79	102

84.2% of cycle iodine remains.

TABLE A.42. Iodine Loading Characteristics for
AgZ Bed 2, Cycle 12, Stripping Stage #1

<u>AgZ Bed Segment</u>	<u>Cycle Loading, g I</u>	<u>Cycle Loading, mg I/g AgZ</u>	<u>Total Loading mg I/g AgZ</u>
1	3.4	85	94
2	5.4	134	144
3	5.9	147	156
4	3.7	92	98
5	3.9	96	108
6	1.8	45	66
7	0.84	21	68
8	0.44	11	81
Total	25.3		
Average		79	102

84.1% of cycle iodine remains.

TABLE A.43. Iodine Loading Characteristics for
AgZ Bed 2, Cycle 12, Stripping Stage #2

<u>AgZ Bed Segment</u>	<u>Cycle Loading, g I</u>	<u>Cycle Loading, mg I/g AgZ</u>	<u>Total Loading mg I/g AgZ</u>
1	3.6	90	99
2	5.2	130	140
3	4.1	103	112
4	2.1	52	58
5	0.54	14	25
6	0.11	3	24
7	0.00	0.0	40
8	0.22	5	75
Total	15.9		
Average		50	72

53.0% of cycle iodine remains.

TABLE A.44. Iodine Loading Characteristics for
AgZ Bed 2, Cycle 12, Stripping Stage #3

<u>AgZ Bed Segment</u>	<u>Cycle Loading, g I</u>	<u>Cycle Loading, mg I/g AgZ</u>	<u>Total Loading mg I/g AgZ</u>
1	6.1	152	161
2	4.0	100	110
3	3.8	95	104
4	1.2	31	37
5	0.090	2	14
6	0.00	0.0	12
7	0.00	0.0	35
8	0.24	6	66
Total	15.5		
Average		48	67

51.6% of cycle iodine remains.

TABLE A.45. Iodine Loading Characteristics for
AgZ Bed 2, Cycle 12, Stripping Stage #4

<u>AgZ Bed Segment</u>	<u>Cycle Loading, g I</u>	<u>Cycle Loading, mg I/g AgZ</u>	<u>Total Loading, mg I/g AgZ</u>
1	3.23	81	89
2	3.74	94	104
3	2.46	62	70
4	0.35	9	15
5	0.14	4	15
6	0	0	0
7	0	0	0
8	0	0	57
Total	10.2		
Average		32	44

•
•
•
•

•
•
•
•

DISTRIBUTION

<u>No. of Copies</u>		<u>No. of Copies</u>
<u>OFFSITE</u>		
27	<u>DOE Technical Information Center</u> R. E. Cunningham Office of Nuclear Safety Materials and Safeguards Room 562 Nuclear Regulatory Commission 7915 Eastern Avenue Silver Springs, MD 20555	8 DOE Office of Defense Waste and Byproducts Management DP-12, GTN Washington, DC 20545 ATTN: A. A. Camacho G. H. Daly J. E. Dieckhoner J. Jicha D. J. McGoff G. Oertel A. L. Taboas V. G. Trice
3	Division of Waste Management Nuclear Regulatory Commission Washington, DC 20910 Attn: J. B. Martin D. B. Rohrer R. D. Smith Materials Section Leader High Level Waste Licensing Branch Nuclear Regulatory Commission Washington, D. C. 20555 W. E. Mott DOE Division of Environmental Control Technology EV-13, GTN Washington, D. C. 20545	Environmental Protection Agency Technological Assessment Division (AW-559) Office of Radiation Programs Washington, DC 20460 S. A. Mann DOE Chicago Operations and Region Office Argonne, IL 60439 J. O. Neff DOE Columbus Program Office 505 King Avenue Columbus, OH 43201
14	DOE Nuclear Waste Management and Fuel Cycle Programs NE30, GTN Washington, D. C. 20545 Attn: W. W. Ballard F. E. Coffman C. R. Cooley H. Feinroth C. H. George O. Gormley M. J. Lawrence J. A. Leary W. H. McVey S. Meyers A. F. Perge R. W. Ramsey, Jr. J. A. Turi R. D. Walton	4 DOE Idaho Operations Office 505 Second Street Idaho Falls, ID 83401 Attn: J. P. Hamric S. Vorndran J. B. Whitsett M. A. Widmayer Office of the Assistant Manager for Energy Research and Development DOE Oak Ridge Operations Office P. O. Box E Oak Ridge, TN 37830
		3 DOE Savannah River Operations Office P.O. Box A Aiken, SC 29801 Attn: E. S. Goldberg T. B. Hindman R. P. Whitfield

No. of
Copies

No. of
Copies

	R. Y. Lowrey DOE Albuquerque Operations Office P.O. Box 5400 Albuquerque, NM 87185		R. Williams Electric Power Research Institute 3412 Hillview Avenue P. O. Box 10412 Palo Alto, CA 94304
	S. G. Harbinson DOE San Francisco Operations Office 1333 Broadway Oakland, CA 94612	4	Exxon Nuclear Idaho P.O. Box 2800 Idaho Falls, ID 83401 ATTN: R. A. Brown J. D. Christian D. L. Condotta T. R. Thomas
	W. F. Holcomb National Institute of Health Radiation Safety Branch Building 21 Bethesda, MD 20205		Los Alamos National Laboratory P. O. Box 1663 Los Alamos, NM 87544
2	Allied-General Nuclear Services P. O. Box 847 Barnwell, SC 29812 ATTN: J. A. Buckham A. Williams	7	Oak Ridge National Laboratory P.O. Box X Oak Ridge, TN 37830 ATTN: R. E. Blanco J. O. Blomeke W. D. Burch A. G. Croff D. E. Ferguson G. L. Haag R. S. Lowrie T. H. Row
3	Argonne National Laboratory 9700 South Cass Avenue Argonne, IL 60439 ATTN: J. H. Kittel L. J. Jardine M. J. Steindler/- L. E. Trevorrow		
10	Battelle Memorial Institute 505 King Avenue Columbus, OH 43201 ATTN: S. H. Basham A. Brandstetter W. Carbiener N. E. Carter J. O. Duguid S. Goldsmith P. L. Hofmann M. Kehnemuyi J. F. Kircher B. Rawles	7	E. I. duPont deNemours & Co. Inc. Savannah River Laboratory Aiken, SC 29801 ATTN: H. H. Baker M. D. Boersma J. L. Crandall S. D. Harris D. L. McIntosh S. Mirshak S. W. O'Rear
2	EG&G Idaho, Inc. P.O. Box 1625 Idaho Falls, ID 83415 ATTN: G. B. Levin R. L. Tallman		E. Vejvoda Rockwell International Rocky Flats Plant P. O. Box 464 Golden, CO 80401

Copies

R. G. Barnes
General Electric Company
175 Curtner Avenue
(M/C 160)
San Jose, CA 95125

L. H. Brooks
Gulf Energy and Environmental
Systems
P. O. Box 81608
San Diego, CA 92138

J. L. Larocca, Chairman
Energy Research and Develop-
ment Authority
Empire State Plaza
Albany, NY 12223

2 Lawrence Livermore Laboratory
P. O. Box 808
Livermore, CA 94550
ATTN: J. H. Campbell
W. G. Sutliff

4 Sandia Laboratories
Albuquerque, NM 87185
ATTN: D. R. Anderson
O. E. Jones
R. G. Kepler
W. Weart

J. W. Bartlett
The Analytic Sciences Corp.
6 Jacob Way
Reading, MA 01867

W. A. Freeby
Bechtel Group, Inc.
Fifty Beale Street
P. O. Box 3965
San Francisco, CA 94119

J. R. Potter
Chem-Nuclear Systems, Inc.
P. O. Box 1866
Bellevue, WA 98009

R. G. Post
College of Engineering
University of Arizona
Tucson, AZ 85721

No. of
Copies

L. L. Hench
Dept. of Materials Science
and Engineering
University of Florida
Gainesville, FL 32611

H. Palmour III
2140 Burlington Engineering
Laboratories
North Carolina State University
Raleigh, NC 27607

W. Tope
Westinghouse Electric Corporation
Penn Center, Building 2
Box 355
Pittsburgh, PA 15230

R. Roy
202 Materials Research Laboratory
University Park, PA 16802

F. K. Pittman
3508 Sagecrest Terrace
Ft. Worth, TX 76109

ONSITE

6 DOE Richland Operations Office

E. A. Bracken
R. D. Gerton
H. E. Ransom
J. J. Schreiber (2)
M. W. Shupe

21 Rockwell Hanford Operations

H. Babad
J. L. Deichman
L. Jensen
R. G. Johnson
J. O. Honeyman
J. E. Kinzer
E. J. Kosiancic
M. P. Larson
G. G. Pitts
I. E. Reep
J. Reser
J. H. Roecker
J. S. Schoefield

No. of
Copies

W. W. Schulz
R. E. Vanderlock
R. Watson
J. R. Wetch
D. G. Wilkins
D. D. Wodrich
G. D. Wright
File copy

UNC United Nuclear Industries

F. H. Bouse, Document Control
T. E. Dabrowski,

Westinghouse Hanford Company

A. G. Blasewitz
R. E. Lerch

78 Pacific Northwest Laboratory

W. F. Bonner
F. P. Brauer
L. A. Bray
L. L. Burger (15)
D. B. Cearlock
T. D. Chikalla
F. H. Dove
H. Drucker
C. E. Elderkin
C. R. Hann
A. J. Haverfield
O. F. Hill
J. H. Jarrett
A. B. Johnson, Jr.
M. R. Kreiter
L. T. Lakey
S. F. Liebetrau
R. C. Liikala
R. P. Marshall
J. L. McElroy
R. W. McKee
J. E. Mendel
J. E. Minor
I. C. Nelson
J. M. Nielsen/R. W. Perkins
R. E. Nightingale
D. E. Olesen
A. M. Platt
J. V. Robinson
W. A. Ross/R. D. Nelson

J. M. Rusin
R. D. Scheele (15)
J. K. Soldat
A. M. Sutey
J. L. Swanson
G. L. Tingey
R. P. Turcotte
C. M. Unruh
H. H. Van Tuyl
B. E. Vaughn
E. C. Watson
E. J. Wheelwright
W. R. Wiley
Technical Information (5)
Publishing Coordination (2)